Tuning of Metal−Metal Bonding and Magnetism via the Electron Count in $Ga_xV_{4-y}Cr_yS_8$

Daniel Bichler and Dirk Johrendt*

Ludwig-Maximilians-Universität München, Department Chemie und Biochemie, Butenandtstrasse 5-13 (Haus D), D-81377 München, Germany

Received March 29, 2007. Revised Manuscript Received May 11, 2007

Mixed crystals of the series $Ga_x(V_{4-y}Cr_y)S_8$ with $x = 1$ and 1.33 and $y = 0-4$ were synthesized and their crystal structures, magnetic and electrical properties were investigated. GaV_4S_8 crystallizes in the $GaMo_4S_8$ structure ($F\bar{4}3m$) containing V_4 clusters and gallium atoms ordered in $^1/_{16}$ of the tetrahedral holes of a face-centered cubic (fcc) sulfur packing. This structure is maintained up to $y \approx 2$ with $(V_{4-y}Cr_y)$ mixed clusters. Higher chromium contents ($y \geq 2$) lead to filling of a second tetrahedral site with Ga atoms ($x > 1$) corresponding to a deficient spinel structure with partial disorder on the gallium sites ($F\bar{4}3m$). Single-crystal structure data prove the lengthening of the metal−metal bonds and the disbanding of the $(V_{4-y}Cr_y)$ clusters around $y \approx 2$. Experimental magnetic moments agree with a cluster molecular orbital (MO) model up to $y \approx 2$ and with separated V^{3+}/Cr^{3+} ions for $y > 2$. Structural and magnetic data both verify the transition from the $GaMo_4S_8$ structure to the spinel type. The destabilization of the clusters in the series $Ga_xV_{4-y}Cr_yS_8$ and the nonexistence of $GaCr_4S_8$ is due to unfavorable spin pairing energy in the cluster MO at $y > 2$, but is also a result of the stability of trivalent chromium in sulfides.

Introduction

Compounds with the $GaMo_4S_8$ structure[1] represent a special class of Mott insulators, where electronic conduction takes place by hopping of electrons between widely separated tetrahedral M_4 clusters (M = transition metal) instead between single atoms as in classical Mott insulators. These materials exhibit interesting structural, magnetic, and electronic properties, among them 4*d*-ferromagnetism,[2,3] phase transitions,[4,5] heavy-fermion behavior,[6] and superconductivity under high pressure.[7,8] One of the first known and most investigated ferromagnetic compounds with $GaMo_4S_8$ structure is GaV_4S_8.[9−14] Apart from the V_4 cluster viewpoint, the structure may also be described as a cation-deficient spinel, where the ordered occupation of half of the tetrahedral sites reduces the space group symmetry from $Fd\bar{3}m$ to $F\bar{4}3m$. A further important difference to the spinel structure is a shift of the vanadium atoms from the centers of the octahedra along [111] toward an empty tetrahedral site. This results in the formation of sulfur-capped tetrahedral V_4 clusters with strong metal−metal bonds and a trigonally antiprismatic coordination of vanadium by sulfur atoms. Since the V−S bonds inside the cluster core are much shorter (about 25 pm) than the bridging ones, we consider the structure as being built up by $V_4S_4^{5+}$ cubes and GaS_4^{5-} tetrahedra arranged in a NaCl-like manner, as shown in Figure 1.

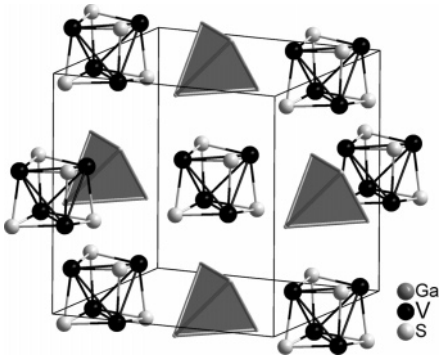

Figure 1. Crystal structure of GaV_4S_8. The $V_4S_4^{5+}$ cubes and GaS_4^{5-} tetrahedra are emphasized.

The formation of M_4 cluster units from a network of equidistant metal atoms in the spinel type, as shown in

* Corresponding author e-mail: Dirk.Johrendt@cup.uni-muenchen.de.

(1) Perrin, C.; Chevrel, R.; Sergent, M. *Comptes Rendus Serie C* **1975**, *280*, 949−951.
(2) Barz, H. *Mater. Res. Bull.* **1973**, *8*, 983−988.
(3) Rastogi, A. K.; Berton, A.; Chaussy, J.; Tournier, R.; Potel, M.; Chevrel, R.; Sergent, M. *J. Low Temp. Phys.* **1983**, *52*, 539−557.
(4) Francois, M.; Lengauer, W.; Yvon, K.; Ben Yaich-Aerrache, H.; Gougeon, P.; Potel, M.; Sergent, M. *Z. Kristallogr.* **1991**, *196*, 111−120.
(5) Müller, H.; Kockelmann, W.; Johrendt, D. *Chem. Mater.* **2006**, *18*, 2174−2180.
(6) Rastogi, A. K.; Wohlfarth, E. P. *Phys. Status Solidi B* **1987**, *142*, 569−573.
(7) Abd-Elmeguid, M. M.; Ni, B.; Khomskii, D. I.; Pocha, R.; Johrendt, D.; Wang, X.; Syassen, K. *Phys. Rev. Lett.* **2004**, *93*, 126403/1−4.
(8) Pocha, R.; Johrendt, D.; Ni, B.; Abd-Elmeguid, M. M. *J. Am. Chem. Soc.* **2005**, *127*, 8732−8740.
(9) Brasen, D.; Vandenberg, J. M.; Robbins, M.; Willens, R. H.; Reed, W. A.; Sherwood, R. C.; Pinder, X. J. *J. Solid State Chem.* **1975**, *13*, 298−303.
(10) Pocha, R.; Johrendt, D.; Pöttgen, R. *Chem. Mater.* **2000**, *12*, 2882−2887.
(11) Haeuseler, H.; Reil, S.; Elitok, E. *Int. J. Inorg. Mater.* **2001**, *3*, 409−412.
(12) Rastogi, A. K.; Niazi, A. *Physica B* **1996**, *223&224*, 588−590.
(13) Sahoo, Y.; Rastogi, A. K. *J. Phys.: Condens. Matter* **1993**, *5*, 5953−5962.
(14) Nakamura, H.; Chudo, H.; Shiga, M. *J. Phys.: Condens. Matter* **2005**, *17*, 6015−6024.

10.1021/cm0708766 CCC: $37.00
Published on Web 07/26/2007

Figure 2, has crucial consequences for the physical properties. The metal-centered electrons not incorporated in *M*−S bonding are now localized in cluster molecular orbitals (MOs). Since the intercluster distances are too long (typically ∼400 pm) for significant orbital overlap, $GaMo_4S_8$-type compounds are narrow-band semiconductors.

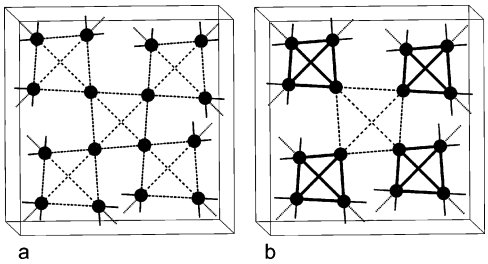

Figure 2. Substructures of the metal atoms in the spinel-type (a) and in the $GaMo_4S_8$ structure (b).

As we reported in recent publications, fundamental physical properties of these compounds such as magnetism and electrical conductivity can be rationalized by a simple cluster molecular orbital scheme.[5,10,15−17] Six *M*−*M* bonding MOs are available for a maximum of 12 metal-centered electrons. GaV_4S_8 contains 7 electrons in each V_4 unit according to the ionic formula splitting $Ga^{3+}(V^{3.25+})_4(S^{2-})_8$, whereas the cluster MO is almost completely filled with 11 electrons in $GaMo_4S_8$. Both MO schemata are depicted in Figure 3.

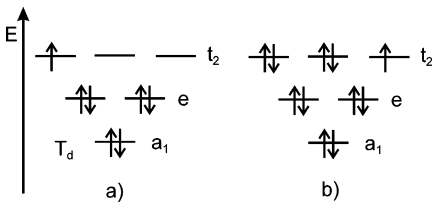

Figure 3. Molecular orbital schemes for the tetrahedral M_4 clusters: (a) GaV_4S_8 and (b) $GaMo_4S_8$.

The highest occupied molecular orbital (HOMO) is threefold degenerated in the cubic case. One spin remains unpaired in this t_2 orbital and causes the magnetic properties of GaV_4S_8 and $GaMo_4S_8$. Experimental magnetic moments are compatible with one spin per V_4 or Mo_4 cluster, respectively, in good agreement with this simple MO scheme. Also, GeV_4S_8 with eight electrons (even number) in the MO follows this model and exhibits the magnetic moment of two spins per V_4 cluster.[5,15] All three compounds mentioned here show ferro- or antiferromagnetic ordering at low temperatures (10−30 K) and are narrow-gap semiconductors ($E_g \approx 0.2$ eV).[5,8,10,15]

The interesting electronic and magnetic properties of the $GaMo_4S_8$ type compounds are in good agreement with the predictions of the cluster MO scheme. From this starting point, we had the idea to increase the electron count in GaV_4S_8 stepwise from 7 to 11 and to study the resulting magnetism. According to the model proposed above, we expected growing magnetic moments up to maximal three unpaired spins in the t_2 level (9 electrons per cluster) followed by a decrease due to spin pairing. Increasing the cluster electron count seemed possible by substituting vanadium gradually by chromium. However, $GaCr_4S_8$ is not known up to now, but the closely related ferromagnetic spinel α-$Ga_{1.33}Cr_4S_8$ with partially ordered occupation of the gallium sites and antiferromagnetic β-$Ga_{1.33}Cr_4S_8$ with random distribution of gallium at the tetrahedral sites are known.[18] In this paper, we report the synthesis, the structural characterization, and the trends of the structural and magnetic properties in the solid solution $Ga_xV_{4-y}Cr_yS_8$.

Experimental Section

Synthesis. Starting materials were gallium ingots (99.999%, Alfa Aesar), vanadium granules (99.5%, Alfa Aesar), chromium powder (99.8%, Alfa Aesar), and sulfur flakes (99.99%, Sigma-Aldrich). Powder samples of $Ga_xV_{4-y}Cr_yS_8$ with $x = 1$ and 1.33 and $y = 0-4$ were prepared by reacting stoichiometric mixtures of the elements in silica tubes under argon atmosphere at 1273 K, heated at a rate of 30 K/h and holding the final temperature for 12 h. After this initial heating, the samples were cooled to room temperature and ground. The process was repeated until homogeneous phases were obtained. This procedure yielded black, crystalline powders, which are not sensitive to air. Small single crystals with metallic luster were selected directly from the samples.

EDX Measurements. Semiquantitative compositions were obtained by energy dispersive X-ray (EDX) analysis using a scanning electron microscope (JEOL JSM-6500 FE-SEM) equipped with an EDX detector (Oxford Instruments). The samples were prepared on a brazen sample holder and coated with carbon to ensure electric conductivity. Several points on the sample were investigated, and the results were averaged (standards: S/FeS_2, V/V, Cr/Cr, and Ga/GaP).

X-ray Powder Diffraction. X-ray powder patterns were recorded using a Stoe Stadi-P diffractometer (Cu $K\alpha_1$ radiation, Ge(111)-monochromator, 7° position sensitive detector, Si as external standard) or a Huber G670 imaging plate diffraction system (Cu $K\alpha_1$ radiation, Ge(111)-monochromator, SiO_2 as external standard). Lattice parameters were refined using the software WinXPow.[19]

Single-Crystal X-ray Diffraction. Crystals from samples of different compositions were selected, glued to thin silica fibers, and checked for their quality by Laue photographs. Suitable specimens were used to collect complete intensity data sets in the oscillation mode with a Stoe IPDS-1 imaging plate detector (Mo $K\alpha$ radiation, graphite monochromator). Data processing and numerical absorption corrections were performed using the X-RED program.[20] The structures were solved with the direct methods program SHELXS[21] and refined with full-matrix least-squares using SHELXL.[22] All final cycles included anisotropic displacement parameters. Because of the practically identical scattering powers of Cr and V, we were unable to refine the V/Cr ratios and have, thus, fixed them to the EDX results. However, certain deviations from the nominal compositions of about ±10% are possible.

Electrical Resistivity. Cold-pressed powder pellets (diameter = 6 mm, height ≈ 1 mm) of the samples were sintered at 1273 K for

(15) Johrendt, D. *Z. Anorg. Allg. Chem.* **1998**, *624*, 952−958.
(16) Shanthi, N.; Sarma, D. D. *J. Solid State Chem.* **1999**, *148*, 143−149.
(17) Le Beuze, A.; Loirat, H.; Zerrouki, M. C.; Lissillour, R. *J. Solid State Chem.* **1995**, *120*, 80−89.
(18) Ben Yaich, H.; Jegaden, J. C.; Potel, M.; Sergent, M.; Huguet, P.; Alquier, G. *Mater. Res. Bull.* **1983**, *18*, 853−860.
(19) *WinXPow* 1.08; STOE & Cie GmbH: Darmstadt, Germany, 2000.
(20) *X-RED32 X-RED Data Reduction*, 1.26; Stoe & Cie GmbH: Darmstadt, Germany, 2004.
(21) *SHELXS*; Sheldrick, G. M., Universität Göttingen: Göttingen, Germany, 1997.
(22) *SHELXL*; Sheldrick, G. M., Universität Göttingen: Göttingen, Germany, 1997.

12 h. The pellets were contacted with silver wires and silver paste, and the electrical resistances were measured between 8 and 320 K using a dc four-point current-reversal method.[23]

Magnetic Measurements. Magnetic properties of the samples were measured utilizing a SQUID magnetometer (MPMS-XL Quantum Design Inc.). Fine ground powder samples were inserted in capsules, and those were fixed into a straw of known diamagnetism. The magnetic susceptibilities of the samples were collected in the temperature range of 1.8 to 300 K with magnetic flux densities up to 5 T. To determine the Curie points, zero-field-cooled and field-cooled measurements at 3 mT were done. The data were corrected for diamagnetic contributions of the capsule, the straw, and the sample using diamagnetic increments[24] and analyzed with a modified Curie−Weiss law:

$$\chi_{mol} = \chi_0 + \frac{C}{T - \Theta}$$

From the Curie constants C, the effective magnetic moments per formula unit were calculated using the spin-only approximation.

Results

Crystal Structures. The X-ray powder patterns of samples with the nominal compositions $Ga(V_{4-y}Cr_y)S_8$ show single phases up to $y \approx 1.5$ and could be indexed using cubic face-centered unit cells. In this range, the lattice parameter changes only slightly from 966.1 pm (GaV_4S_8) to 968.0 pm ($Ga(V_{2.5}Cr_{1.5})S_8$) as expected from the similar ionic radii of vanadium and chromium. But the lattice parameter grows rapidly around $y \approx 2$, reaches 986.7 pm at $y = 2.5$, and remains around 989 pm up to $y = 4$. The lattice parameters are listed in Table 1 and graphically depicted in Figure 4.

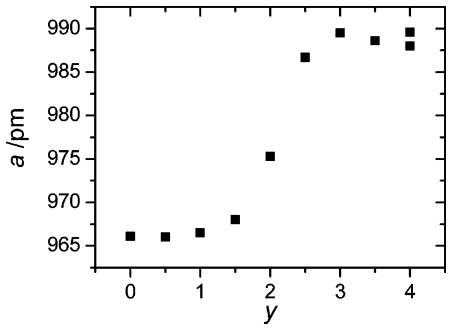

Figure 4. Lattice parameters of the series $Ga_x(V_{4-y}Cr_y)S_8$. The two symbols at $y = 4$ mark the α- and β-polymorphs of $Ga_{1.33}Cr_4S_8$.[18]

Noticeable amounts of impurity phases—mainly Cr_2S_3—were initially detected for $y \geq 2$, indicating that these compounds may not have the nominal composition $Ga(V_{4-y}Cr_y)S_8$. For that reason, we performed X-ray structure determinations of single crystals selected from samples with $y = 1.5$, 2.0, and 2.5. Parameters of the data collections and results of the structure refinements together with selected bond distances are compiled in Table 2. Further details of the crystal structure determinations (CIF data) are deposited and can be obtained from Fachinformationszentrum Karlsruhe, D-76344 Eggenstein-Leopoldshafen (Germany)

(23) *Keithley Low Level Measurements, Precision DC Current, Voltage and Resistance Measurements*, 5th ed.; Keithley Instruments, Inc.: Cleveland, OH, 1998.

(24) Lueken, H. *Magnetochemie*; Teubner: Stuttgart, Leipzig, Germany, 1999.

Table 1. Lattice Parameters of the Series $Ga_x(V_{4-y}Cr_y)S_8$ from Powder Diffraction Data

x	*y*	*a*/pm
1.00	0	966.1(1)
1.00	0.5	966.0(1)
1.00	1	966.5(1)
1.00	1.5	968.0(3)
1.10	2	975.3(5)
1.33	2.5	986.7(10)
1.33	3	989.5(2)
1.33	3.5	988.6(2)
1.33	4 (α)	989.6[a]
1.33	4 (β)	988.0[a]

[a] Lattice parameters from ref 18.

(e-mail: crysdata@fiz-karlsruhe.de), by quoting the Registry No.'s 417903 ($Ga(V_{2.5}Cr_{1.5})S_8$), 417904 ($Ga_{1.11}(V_2Cr_2)S_8$), and 417905 ($Ga_{1.33}V_{1.5}Cr_{2.5}S_8$).

The refinements confirmed the $GaMo_4S_8$-type structure for $Ga(V_{2.5}Cr_{1.5})S_8$ with space group $F\bar{4}3m$, and we can safely assume that this is also the case for all compounds with $y < 1.5$. For $y = 2$, we detected weak electron density at a second tetrahedral site (4*c*), which is empty in the $GaMo_4S_8$ structure. We refined the structure still in the space group $F\bar{4}3m$ with ~10% gallium atoms occupying this position. Apart from the Cr/V statistics, this is essentially the structure of α-$Ga_{1.33}Cr_4S_8$, but with lower Ga content of 0.11 at the second tetrahedral site (4*c*). The occupation of this site increases to 0.33 in the crystal with nominal composition $y = 2.5$. Simultaneously, the distances within the $(V_{4-y}Cr_y)$ clusters increase from 291 pm at $y = 0-1.5$ to 306 pm at $y = 2$ and reach 325 pm for $y = 2.5$. The latter is too long to be considered as a significant metal−metal bond. This alteration of the $M-M$ distances within and between the clusters is depicted in Figure 5. Obviously, the $GaMo_4S_8$ structure exists up to a composition close to $Ga(V_2Cr_2)S_8$ with nine electrons in the cluster orbitals.

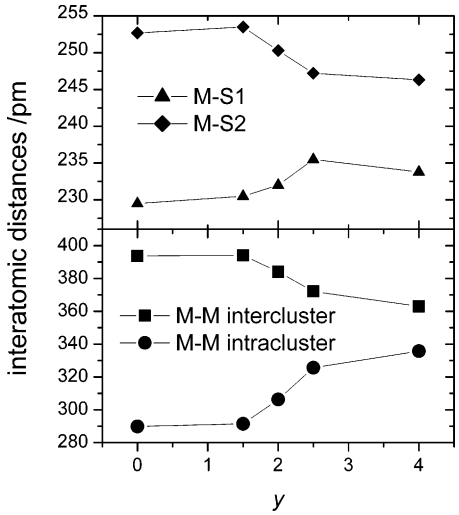

Figure 5. M−S and $M-M$ (M = V/Cr) distances in the series $Ga_xV_{4-y}Cr_yS_8$.

The chemical compositions obtained from the single-crystal data were subsequently used to synthesize phase-pure samples of $Ga_xV_{4-y}Cr_yS_8$ with $x = 1.1-1.33$ and $y \geq 2$. Their X-ray powder patterns were free from reflections of Cr_2S_3 or other impurity phases and suitable for magnetic measurements.

Table 2. Crystallographic Data and Details of the Data Collections for $Ga_xV_{4-y}Cr_yS_8$

chemical formula	$Ga(V_{2.5}Cr_{1.5})S_8$	$Ga_{1.11}(V_2Cr_2)S_8$	$Ga_{1.33}V_{1.5}Cr_{2.5}S_8$
M_r	531.55	539.83	553.18
cell setting, space group	cubic, $F\bar{4}3m$	cubic, $F\bar{4}3m$	cubic, $F\bar{4}3m$
temperature /K	293(2)	293(2)	293 (2)
a/pm	969.5(2)	976.3(2)	986.7(2)
$V/10^6$ pm^3	911.3(2)	930.7(2)	960.5(2)
Z	4	4	4
Dx /Mg m^{-3}	3.874	3.852	3.825
radiation type	Mo Kα	Mo Kα	Mo Kα
μ /mm^{-1}	8.88	9.09	9.39
diffractometer	STOE IPDS-1	STOE IPDS-1	STOE IPDS-1
data-collection method	oscillation	oscillation	oscillation
absorption correction	numerical	numerical	numerical
T_{min}	0.546	0.547	0.635
T_{max}	0.626	0.610	0.677
no. of measured, indep. observed reflections	2118, 214, 210	1631, 173, 171	1882, 182, 160
R_{int}	0.049	0.034	0.054
θ_{max} /°	32.9	29.9	30.3
$R[F^2 > 2\sigma(F^2)]$, $wR(F^2)$, *S*	0.038, 0.101, 1.11	0.018, 0.043, 1.09	0.032, 0.072, 1.09
no. of reflections	214 reflections	173 reflections	182 reflections
no. of parameters	13	14	13
$(\Delta/\sigma)_{max}$	<0.0001	<0.0001	<0.0001
$\Delta\rho_{max}$, $\Delta\rho_{min}$ /e Å^{-3}	1.41, −1.34	0.39, −0.32	0.62, −0.75
extinction coefficient	0.0037 (9)	−	−
Flack parameter	−	−	0.09 (6)
twin ratio	0.56 (7)	0.68 (3)	−
atomic parameters	4 Ga1 on 4a (0, 0, 0)	4 Ga1 on 4a (0, 0, 0)	4 Ga1 on 4a (0, 0, 0)
		0.44(3) Ga2 on 4*c*	1.23(4) Ga2 on 4*c*
		($^1/_4$, $^1/_4$, $^1/_4$)	($^1/_4$, $^1/_4$, $^1/_4$)
	6 Cr/10 V on 16*e* (*x*, *x*, *x*)	8 Cr/8 V on 16*e* (*x*, *x*, *x*)	10 Cr/ 6 V on 16*e* (*x*, *x*, *x*)
	$x = 0.6063(1)$	$x = 0.6110(1)$	$x = 0.6166(2)$
	16 S1 on 16*e* (*x*, *x*, *x*)	16 S1 on 16*e* (*x*, *x*, *x*)	16 S1 on 16*e* (*x*, *x*, *x*)
	$x = 0.8644(2)$	$x = 0.8650(1)$	$x = 0.8659(2)$
	16 S2 on 16*e* (*x*, *x*, *x*)	16 S2 on 16*e* (*x*, *x*, *x*)	16 S2 on 16*e* (*x*, *x*, *x*)
	$x = 0.3707(2)$	$x = 0.3743(1)$	$x = 0.3781(2)$
selected distances /pm			
Ga1-S1	227.8(2)	228.3(2)	229.1(3)
Ga2-S2		210.1(2)	218.9(3)
M-S2	230.5(2)	232.0(1)	235.4(2)
M-S1	253.4(2)	250.3(1)	247.3(2)
intercluster *M*−*M* distances	291.4(3)	306.4(2)	325.3(5)
intracluster *M*−*M* distances	394.1(3)	384.0(2)	372.4(5)

Table 3. Magnetic Data of the Series $Ga_xV_{4-y}Cr_yS_8$; Experimental Effective Magnetic Moments are Compared with Values Calculated from the Cluster MO Model (M_4) or for Separated M^{3+} Ions.

		μ_{eff}/μ_B per f.u. (±0.05)			no. unpaired e$^-$/M_4		magnetic ordering		
x	*y*	exp.	calc. M_4	calc. M^{3+}	exp.	calc.	T_C/K	Θ/K	χ_0 [c]
1.0	0.0	1.74	1.73	5.7	1.0	1.0	10(1)	−31(4)	0.2
1.0	0.5	2.02	2.29	6.0	1.3	1.5	10(1)	11(2)	2.0
1.0	1.0	2.67	2.83	6.2	1.9	2.0	10(1)	8(1)	2.0
1.0	1.5	3.26	3.35	6.6	2.4	2.5	10(1)	9(2)	2.0
1.1	2.0	4.18	3.87	6.8	3.3	3.0	5(1)	9(1)	3.0
1.33	2.5	5.62	3.35	7.0	a	2.5	*b*	−17(1)	0.0
1.33	3.0	6.11	2.83	7.3	a	2.0	15(1)	1(2)	4.0
1.33	3.5	6.19	2.29	7.5	a	1.5	14(1)	1(1)	1.0
1.33	4.0	7.06[d]	1.73	7.74	a	1.0	30[d]	20[d]	

[a] Spinel-like structure. [b] No ordering detected at $T > 2$ K. [c] $\pm 0.1/10^{-8}$ m^3 mol^{-1}. [d] From ref 25.

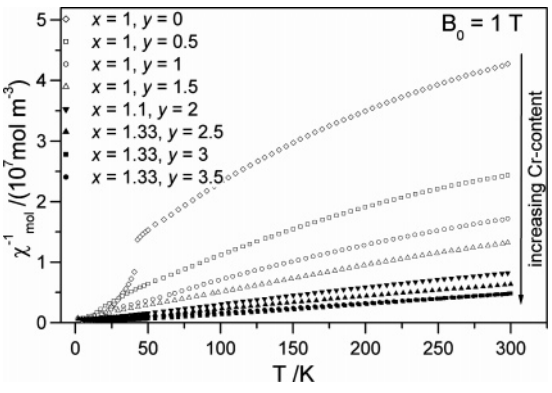

Figure 6. Inverse magnetic susceptibilities of $Ga_xV_{4-y}Cr_yS_8$.

Magnetism. The temperature dependencies of the magnetic susceptibilities are shown in Figure 6, and the complete magnetic data are summarized in Table 3. It is evident that the magnetic moments rise with increasing chromium content. The sudden drop of the χ(T) curve of GaV_4S_8 at ~38 K comes from a structural transition from cubic to rhombohedral symmetry, which is no longer observed in the mixed crystals. The expected magnetic moment of one unpaired electron per V_4-cluster has been reported for GaV_4S_8[10] and verified in the present work. Each chromium adds one electron to the t_2 levels of the cluster MO (see Figure 2), and the effective moments should be compatible with one, two, or three unpaired spins, respectively, according

to the Hund rule. Indeed, for the vanadium richer compounds up to $y = 2$, the magnetic susceptibilities can be nicely explained by the cluster orbital picture. We find moments compatible with $1 + y$ unpaired electrons in good agreement with this model (see Table 3). But this does not hold true for the chromium richer part with $y > 2$. Instead of decreasing moments due to spin pairing in the t_2 orbitals, we now observe further increasing effective moments. These values can be better rationalized by assuming separated Cr^{3+}/V^{3+} ions than by the M_4 cluster model.

Figure 7 shows the behavior of the magnetic moments in the series $Ga_xV_{4-y}Cr_yS_8$ graphically. The agreement with the cluster MO model is evident up to $y \approx 2$. For $y > 2$, the experimental effective magnetic moments increase strongly and are closer to those expected theoretically for separated ions. However, the measured moments still stay behind the theoretical ones for separated M^{3+} ions. This could be due to inhomogeneities of the samples (remaining amounts of M_4 clusters) or to unknown orbital contributions to the magnetic moments (the values were calculated using the spin-only approximation). Nonetheless, our magnetic data clearly supports the structural results, namely, the disbanding of the M_4 cluster units under reformation of the spinel-like structure without metal−metal bonds.

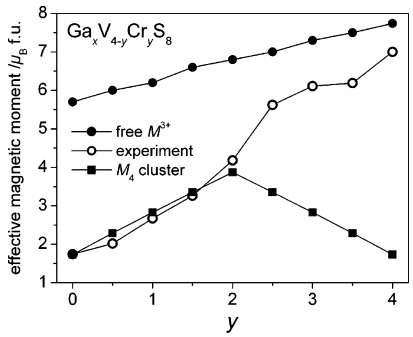

Figure 7. Effective magnetic moments of $Ga_xV_{4-y}Cr_yS_8$ compared with theoretical values expected for separated M^{3+} ions and from the cluster MO model.

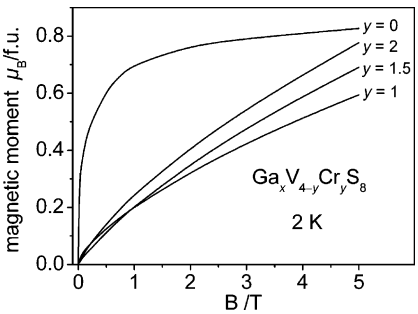

Figure 8. Magnetization isotherms of $Ga_xV_{4-y}Cr_yS_8$ with $y = 0$, 1, 1.5, and 2 at $T = 2$ K.

Selected magnetization isotherms of the $Ga_xV_{4-y}Cr_yS_8$ compounds with ($V_{4-y}Cr_y$) clusters are depicted in Figure 8. GaV_4S_8 shows ferromagnetic order below $T_C = 10$ K, as reported previously.[10] The magnetization at the maximum field (5 T) reaches 0.82 μ_B per V_4 cluster, which is somewhat smaller than the expected 1 μ_B. Remarkably, the negative Weiss constant of −31 K indicates rather antiferromagnetic correlations in the paramagnetic phase. But this is only valid down to 38 K, where the known structural phase transition occurs in GaV_4S_8. This is clearly visible by the sudden drop in the $\chi^{-1}(T)$ plot (Figure 7), which is consistent with vanishing antiferromagnetic correlations. As the chromium content increases, the phase transition is no longer present and the Θ-values becomes positive. We observe ferromagnetic ordering up to $y = 2$, but no saturation of the magnetic moments could be achieved at 5 T. This may be due to decreasing Curie temperatures going down to 5 K for $y = 2$. No magnetic ordering was found in $Ga_{1.3}V_{1.5}Cr_{2.5}S_8$. For the spinel-type compounds with $y \geq 3$, ferromagnetic ordering was again observed with $T_C \approx 14-15$ K. This is lower than the T_C of 30 K as reported for β-$Ga_{1.33}Cr_4S_8$ in ref. 25, which may be due to different methods for determining T_C. If we use this method (inflection point of the susceptibilities temperature dependence) for compounds with $y > 3$, we get $T_C = 25-27$ K as well. However, the experimental susceptibilities already deviate from the Curie−Weiss law below 25−27 K, and this may be considered as the onset of magnetic ordering. Nonetheless, irreversible magnetic behavior in zero-field-cooled/field-cooled cycles as typical for ferromagnetic ordering occurs only below 14−15 K.

Electrical Resistivity. Figure 9 shows the temperature dependencies of the electrical resistances. Semiconducting behavior is observed for different compositions of $Ga_xV_{4-y}Cr_yS_8$. The room-temperature specific resistivities are about 10^{-3} Ω cm and increase exponentially by 5 orders of magnitude to 10^2 Ω cm at 40−60 K. Narrow band gaps about 0.2 eV were obtained from Arrhenius plots between 150 and 320 K. Toward lower temperatures, we observe the apparent decrease of the gap as typical for Mott insulators. The insert in Figure 9 shows the plot of $-\ln(\sigma)$ against $T^{-1/2}$. The linear relation at least below 0.1 (above 100 K) is typical for Mott insulators with variable range hopping (VRH) conductivity.

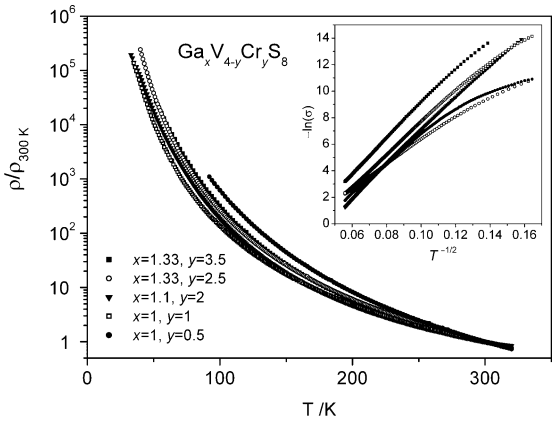

Figure 9. Electrical resistances of $Ga_xV_{4-y}Cr_yS_8$ pellets. The room-temperature specific resistivities are ∼10^{-3} Ω cm, and the band gaps are ∼0.2 eV.

Discussion

The X-ray powder and single-crystal data of the series $Ga_xV_{4-y}Cr_yS_8$ show clearly that the rapid growth of the lattice parameter at $y \approx 2$ is connected with introducing additional gallium atoms at the second tetrahedral site 4*c*. At the same

(25) Nakatani, I. *J. Solid State Chem.* **1980**, *35*, 50−58.

time, we observe the disbanding of the $(V_{4-y}Cr_y)$ cluster units of the $GaMo_4S_8$ structure and the transition to the spinel-type with isolated vanadium and chromium atoms (see Figure 2). The transition is accompanied by a reduction of the formal mean oxidation state from $(Cr/V)^{3.25+}$ in the cluster compounds $Ga(V_{4-y}Cr_y)S_8$ to Cr^{3+} in spinel-like $Ga_{1.33}Cr_4S_8$. Thus, by growing y values, an increasing part of chromium atoms (up to $^1/_4$ in a theoretical $GaCr_4S_8$) must be Cr^{4+}. It is well-known that tetravalent chromium is rather unstable and appears, if at all, extraordinarily rarely in sulfides. CrS_2 itself is unknown and could only be stabilized by charge transfer in layers of misfit structures.[26] The binary sulfide $Cr_{5+x}S_8$ contains <10% Cr^{4+}, and the probably only pure Cr^{4+} sulfide compound seems to be Ba_3CrS_5.[27,28] Both compounds were synthesized under high-pressure conditions. In contrast to this, trivalent chromium is very stable and known to be the favored oxidation state, by far, in sulfides. Besides the strong tendency of chromium to be trivalent, we suggest a second reason for the destabilization of the $(V_{4-y}Cr_y)$ cluster. Just around the critical value $y \approx 2$, we have 9 electrons in the MO (Figure 2) in agreement with our experimental magnetic moments compatible with $S = 3/2$ per cluster. Each t_2 level contains one unpaired spin, and any further increase of the electron count ($y > 2$) would require spin pairing if the cluster was preserved. But the spin pairing costs energy and destabilizes the cluster increasingly when occupied with 10 or 11 electrons as in hypothetical $GaCr_4S_8$. Altogether, the observed structural transformation within the $Ga_xV_{4-y}Cr_yS_8$ series around $y \approx 2$ is driven by electronic effects regarding both oxidation states as well as magnetic correlations inside the cluster MO.

Conclusion

The series $Ga_xV_{4-y}Cr_yS_8$ undergoes a gradual transition from the $GaMo_4S_8$ structure ($x = 1$, $y = 0-2$) to the spinel structure ($x = 1.1-1.33$, $y = 2-4$). This is accompanied with disbanding of the tetrahedral $(V_{4-y}Cr_y)$ cluster units into separated V^{3+}/Cr^{3+} ions and with switching of the magnetism from unpaired spins in cluster MO to classical localized 3*d* moments of separated ions. Interestingly, we find the borderline between the structure types close to $GaV_2Cr_2S_8$, where the maximum of three unpaired spins occupy the t_2 level of the cluster MO. Adding more electrons by higher Cr-contents would require spin pairing, which is energetically unfavorable. $GaCr_4S_8$ could not be obtained, which is suspected because of both avoided spin pairing and the instability of Cr^{4+}. Within the series $Ga_xV_{4-y}Cr_yS_8$, both effects compete with the $M-M$ bonding energy until the spin paring energy in the t_2 orbitals is the decisive factor that destabilizes the $GaMo_4S_8$ structure at least with 3*d* transition elements.

Acknowledgment. This work was financially supported by the Deutsche Forschungsgemeinschaft (DFG) Project Jo257/4-1.

CM0708766

(26) Cario, L.; Johrendt, D.; Lafond, A.; Felser, C.; Meerschhaut, A.; Rouxel, J. *Phys. Rev. B* **1997**, *55*, 9409−9414.
(27) Bensch, W.; Lühmann, H.; Näther, C.; Huppertz, H. *Z. Kristallogr*. **2002**, *217*, 510−514.
(28) Fukuoka, H.; Miyaki, Y.; Yamanaka, S. *J. Solid State Chem.* **2003**, *176*, 206−212.